Taylor & Francis
Taylor & Francis Group

SPECIAL ISSUE IN HONOUR OF TIM SOFTLEY

OPEN ACCESS   Check for updates

Direct excitation of the spin-orbit forbidden $X\,^2\Pi_{3/2} \leftarrow X\,^2\Pi_{1/2}$ transition in NO using the intra-cavity free electron laser FELICE

Theo Cremers [a], Simon Chefdeville[a], Joost M. Bakker [b], W. Leo Meerts[b] and
Sebastiaan Y. T. van de Meerakker[a]

[a]Institute for Molecules and Materials, Radboud University, Nijmegen, Netherlands; [b]Institute for Molecules and Materials, FELIX Laboratory, Radboud University, Nijmegen, Netherlands

ABSTRACT

We present the direct far-infrared optical excitation of NO radicals from the $X\,^2\Pi_{1/2}$ electronic ground state to the $X\,^2\Pi_{3/2}$ spin-orbit excited state. This spin-orbit forbidden transition at a photon energy near 125 cm^{-1} borrows intensity by a small admixture of $^2\Pi_{1/2}$ character into the $^2\Pi_{3/2}$ wavefunction, and can be saturated using the intracavity free electron laser FELICE. In the $X\,^2\Pi_{1/2}$ state, the NO radical has a negligible magnetic moment, whereas the radicals have a large magnetic moment in the $X\,^2\Pi_{3/2}$ excited state. The direct optical excitation demonstrated here thus effectively 'switches on' the molecule's magnetic moment, and allows for the production of a sample of NO ($X\,^2\Pi_{3/2}$) with almost perfect quantum state purity. These optically prepared well-defined packets of magnetic NO radicals offer interesting prospects for the use of this benchmark molecule in molecular deceleration and trapping experiments.
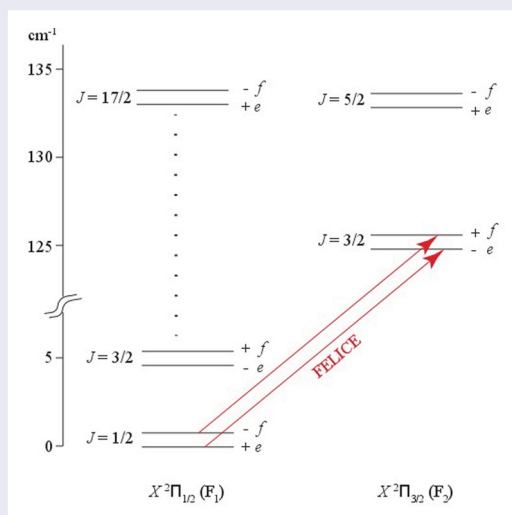
1. Introduction

In the last years, methods have been developed to achieve complete control over molecules in a beam. In particular, Stark and Zeeman decelerators have been constructed with which the velocity of molecules in a beam can be tuned, analogous to the control of charged particles in a linear accelerator [1]. The decelerator selects a part of a molecular beam pulse and accelerates or decelerates this part, producing bunches of molecules with a computer-controlled velocity and with longitudinal temperatures as low as a few mK. The molecular packets that emerge from the decelerator have small spatial and velocity spreads, and have almost perfect quantum state purity.

These 'tamed molecular beams' are ideal starting points for a variety of experiments. Molecules decelerated to a near standstill, for instance, can be loaded

---

CONTACT Sebastiaan Y. T. van de Meerakker   basvdm@science.ru.nl   Radboud University, Institute for Molecules and Materials, Heyendaalseweg 135, 6525 AJ Nijmegen, Netherlands

and confined in traps for times up to seconds [2–4]. This can be used to measure the lifetimes of long-lived excited states [5], or to study collision processes between the trapped molecules at (ultra)low temperatures [6,7]. Slowly moving molecules can also be used in high-resolution spectroscopy and metrology, taking advantage of the increased interaction times resulting in improved spectral resolutions [8,9]. Last but not least, decelerated beams are used in controlled crossed molecular beam scattering experiments, where the tunability of the velocity and narrow velocity spreads are exploited to unravel, with unprecedented accuracy and sensitivity, details of scattering processes that remain elusive in scattering experiments that use conventional beams [10].

One of the most attractive molecular candidates to use in experiments using a Stark or Zeeman decelerator is the NO radical. Its open-shell structure combined with the experimental ease in the generation of dense beams and sensitive detection makes the NO radical a benchmark species in crossed beam and gas-surface scattering experiments alike [11]. Interactions of NO with atoms, for instance, are governed by two potential energy surfaces, yielding the possibility to study molecular collision dynamics beyond the Born-Oppenheimer approximation [12]. In scattering with surfaces, the NO radical has been key to elucidate the role of non-adiabaticity in molecule-surface interactions [13,14].

Unfortunately, however, the NO radical is not very amenable to molecular deceleration. It has only a very small electric dipole moment of 0.16 D, rendering Stark deceleration to a wide range of velocities impractical [15]. In the $X\,^2\Pi_{1/2}$ electronic ground state, the NO radical possesses almost zero magnetic moment, as the magnetic moment of the orbital angular momentum is precisely counteracted by the magnetic moment generated by the electron spin; only a very small magnetic moment arises due to the rotational angular momentum [16]. Therefore, NO radicals in their ground state are largely immune to external magnetic fields, and cannot be decelerated or accelerated in a Zeeman decelerator. By contrast, the orbital and spin angular momenta are oriented in the same direction in the $X\,^2\Pi_{3/2}$ spin-orbit excited state, inducing a large magnetic moment. NO radicals in this state would be excellent candidates for Zeeman deceleration, however, this state is located some $125\,\mathrm{cm}^{-1}$ above the $^2\Pi_{1/2}$ state and hardly populated in a molecular beam. The $^2\Pi_{3/2}$ state can be populated through Franck Condon or stimulated emission pumping via the $A\,^2\Sigma^+$ electronically excited state [17,18], but competition with spontaneous emission to a large number of vibrational states may dilute the quantum state purity in the prepared sample.

Here, we demonstrate the direct and rotationally resolved optical excitation of NO radicals from the $X\,^2\Pi_{1/2}, v'' = 0, J'' = 1/2$ to the $X\,^2\Pi_{3/2}, v' = 0, J' = 3/2$ state. The $X\,^2\Pi_{3/2} \leftarrow X\,^2\Pi_{1/2}$ transition is in principle electric dipole forbidden, but has a non-zero transition strength due to a mixing of $^2\Pi_{1/2}$ character into the $^2\Pi_{3/2}$ wavefunction. We were able to saturate the transition using the Free Electron Laser for Intra-Cavity Experiments FELICE, that allows for the interaction of a molecular beam with Infrared (IR) light inside the cavity of a Free Electron Laser (FEL). The direct optical transfer from the $^2\Pi_{1/2}$ to the $^2\Pi_{3/2}$ state effectively 'switches on' the magnetic moment of the NO radical, and yields a well-defined packet of molecules with high density and excellent quantum state purity that is an ideal starting point for further beam control using, for instance, a Zeeman decelerator.

2. Experiment

The experiments were performed on the FELICE beam line of the Free-Electron Laser for Infrared eXperiments (FELIX) Laboratory at Radboud University, Nijmegen, the Netherlands. The NO beam is obtained by expanding a mixture of NO (5%) seeded in Ar, with a stagnation pressure of approximately 1 bar and at room temperature, into a vacuum chamber using a Nijmegen Pulsed Valve [19]. The beam passes through a skimmer (Beam Dynamics, 1 mm), a differentially pumped vacuum chamber and subsequently enters a third differentially pumped vacuum chamber where it interacts with the IR radiation at a wavelength around $80\,\mu m$ [20]. FELICE produces light in an approximately 10 μs long pulse train of transform-limited picosecond IR laser pulses. The spectral bandwidth can be adjusted between 0.3% and 2% of the laser wavelength, translating into a full-width at half-maximum of 0.4–2.5 cm^{-1} at $125\,\mathrm{cm}^{-1}$.

The NO radicals are state-selectively ionised using a (1+1) REMPI scheme via the $A\,^2\Sigma^+$ state using a pulsed dye laser producing ultra-violet (UV) radiation around 226 nm. The IR pump and UV probe lasers spatially overlap with each other some 20 cm downstream from the skimmer [20]. The dye laser is synchronised to the macropulse of the FEL such that it fires a few microseconds afterwards. The NO ions are extracted by a set of high voltage plate electrodes into a reflectron time-of-flight-mass spectrometer and detected with a Micro-Channel Plate (MCP) detector. The 226 nm radiation is obtained by frequency-doubling a Nd-YAG pumped pulsed dye laser. The signal is measured by integrating the ion time-of-flight mass peak corresponding to the NO ions.
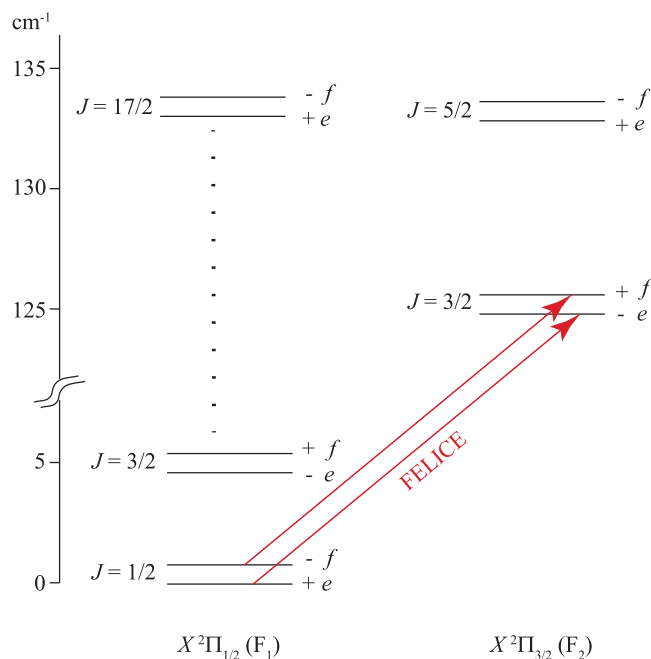
Figure 1. Energy level diagram of the $X^2\Pi$ electronic ground state of NO. Two spin-orbit manifolds exist that are labelled by F_1 and F_2. In both manifolds, each rotational level is spit into two Λ-doublet components. The splitting between both components is largely exaggerated for reasons of clarity. The transitions induced by the FELICE laser are indicated by the arrows.

The energy level scheme of the $X^2\Pi$ electronic ground state of NO is schematically represented in Figure 1. Following standard spectroscopic nomenclature, the $X^2\Pi_{1/2}$ and $X^2\Pi_{3/2}$ manifolds are denoted hereafter as F_1 and F_2, respectively. Each spin-orbit manifold possesses a set of rotational levels, indicated by the quantum number J. The rotational ground states within the F_1 and F_2 manifolds are $J = 1/2$ and $J = 3/2$, respectively. Each rotational level is split into two Λ-doublet components of opposite parity. The Λ-doublet splitting amounts to 318 and 39 MHz for the $F_1, J = 1/2$ and $F_2, J = 3/2$ levels, respectively [21]. The $+$ and $-$, as well as the e and f parity labels are indicated for each level.

Figure 2(a) shows the $A \leftarrow X$ REMPI spectrum of the NO radical measured in absence of interaction with the IR laser. Transitions at photon frequency around 44,200 cm^{-1} (panel b) originate from NO radicals residing in the F_1 manifold. The three main transitions originate from population in the $F_1, J = 1/2, e$ and $F_1, J = 1/2, f$ levels that are equally populated in the molecular beam. Smaller peaks corresponding to the rotationally excited $F_1, J = 3/2, e$ and $F_1, J = 3/2, f$ levels are also visible. From the relative peak intensities, the rotational temperature of the molecular beam is evaluated to be around 2 K. Transitions originating from population in the F_2 levels are located at photon frequencies below

44,100 cm^{-1}, and the REMPI spectrum that is taken when the IR laser is off is shown in the lower curve of panel c. The absence of observed peaks in this energy region indicates that initial population in any of the F_2 levels is negligible.

To excite NO radicals from the F_1 into the F_2 manifold, FELICE was first used in narrow-band mode. The UV laser wavelength was set to probe the population in the $J = 3/2, f$ level of the F_2 manifold, while the FELICE frequency was scanned from 115 to 130 cm^{-1}. The resulting IR spectrum is shown in Figure 2(b), and features a single peak around 124 cm^{-1} corresponding to the $F_2, v = 0, J = 3/2 \leftarrow F_1, v = 0, J = 1/2$ transition. Transitions from individual Λ-doublet components of the initial rotational level are not resolved. No transitions are observed that originate from the $F_1, J = 3/2$ levels that are marginally populated in the molecular beam. These transitions are expected at 119.9 and 128.5 cm^{-1}. The origin of the small feature found around 122 cm^{-1} is at present unclear, but may well originate from the mode structure of FELICE.

The upper trace in Figure 2(c) shows the UV probe spectrum that was recorded when the FELICE pump beam was set to the frequency where the maximum of the $F_2, v = 0, J = 3/2 \leftarrow F_1, v = 0, J = 1/2$ IR transition was observed. Four transitions are observed that probe the population in individual e and f components of the $F_2(3/2)$ level as indicated in the spectrum. No transitions are observed that originate from rotationally excited states within the F_2 manifold, indicating that the direct optical $F_2 \leftarrow F_1$ excitation presented here results in a packet of spin-orbit excited NO (F_2) radicals with excellent quantum state purity.

In order to determine the maximum fraction of NO radicals that can be excited by the IR pump pulse, we operated FELICE at maximum power in broad band mode. Figure 2(d) shows the IR spectrum that was recorded when the UV laser was set to probe the population in the $F_1, J = 3/2, f$ ground state. Depletion of this population by up to 50% was observed, indicating that we can induce the $F_2 \leftarrow F_1$ transition in NO under saturated conditions.

3. Theory

The $X^2\Pi_{3/2} \leftarrow X^2\Pi_{1/2}$ transition is inherently an electric dipole forbidden transition, as the selection rules only support transitions with $\Delta\Omega = 0$, where $\Omega = \Lambda + \Sigma$, the projections of the orbital angular momentum and spin angular momentum on the internuclear axis. In Hund's case (a) the projection of the total angular momentum J on the nuclear axis is Ω. However, there are terms in the rotational Hamiltonian that mix the $^2\Pi_{1/2}$
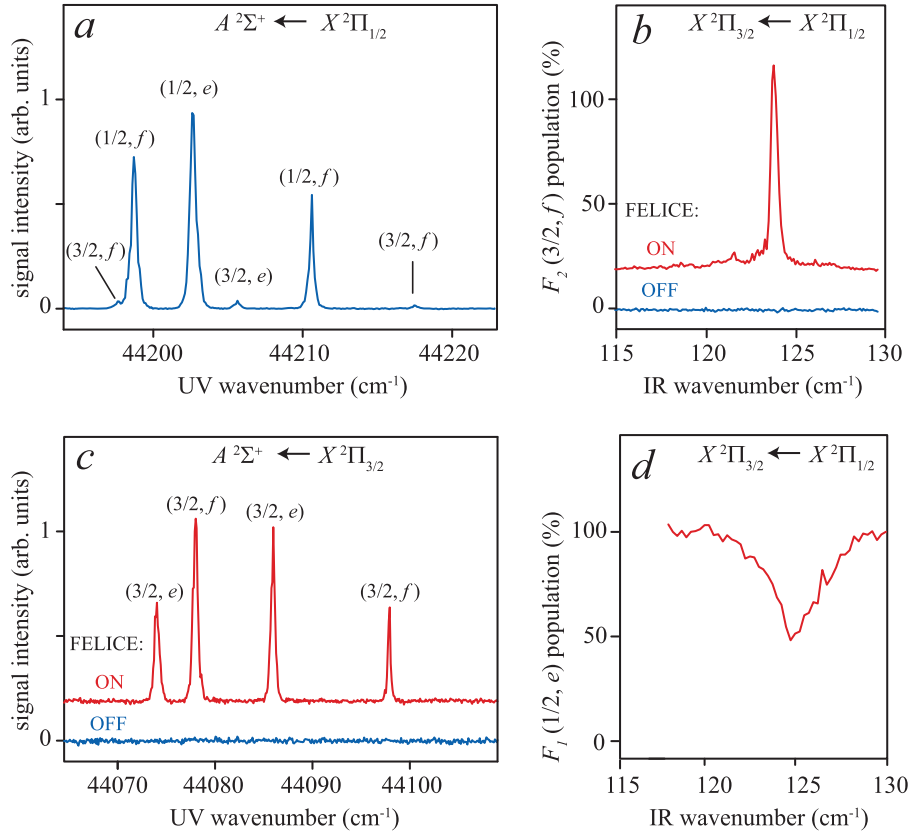
Figure 2. (a) UV excitation spectrum of the $A\,^2\Sigma^+ \leftarrow X\,^2\Pi_{1/2}$ transition in NO. (b) Population in the $X\,^2\Pi_{3/2}, J = 3/2, f$ level as a function of the FELICE photon frequency, without (lower trace) and with IR irradiation (upper trace). The two curves are vertically offset for reasons of clarity. (c) UV excitation spectrum of the $A\,^2\Sigma^+ \leftarrow X\,^2\Pi_{3/2}$ transition in NO, without (lower trace) and with IR irradiation at $125\,\mathrm{cm}^{-1}$ (upper trace). (d) Population in the $X\,^2\Pi_{1/2}, J = 1/2, f$ level as a function of the FELICE photon frequency.

and $^2\Pi_{3/2}$ states. The rotational wavefunctions $|F_i, J\rangle$ within the F_1 and F_2 manifolds can be written as:

$$|F_1, J\rangle = a_J|\Pi_{1/2}, J\rangle - b_J|\Pi_{3/2}, J\rangle$$
$$|F_2, J\rangle = b_J|\Pi_{1/2}, J\rangle + a_J|\Pi_{3/2}, J\rangle, \qquad (1)$$

where $|\Pi_\Omega, J\rangle$ are the pure Hund's case (a) wavefunctions $|J\Lambda\Sigma\Omega\rangle$ with $|\Lambda| = 1$ and $|\Sigma| = 1/2$. Expressions for the mixing coefficients a_J and b_J can be found in ref. [22], and take the values 1.00 and 0.00 for the $F_1, J = 1/2$ state and 0.9997 and 0.0245 for the $F_2, J = 3/2$ state, respectively. Note that in Equation (1) we have not included parity in the wavefunctions that are relevant to denote the Λ-doublet components, as the IR laser bandwidth is insufficiently narrow to resolve individual transitions between Λ-doublet levels. Parity is easily included in the wavefunction by using symmetry-adapted wavefunctions $|\Pi_\Omega^\pm, J\rangle = 1/\sqrt{2}[|J\Lambda\Sigma\Omega\rangle \pm |J - \Lambda - \Sigma - \Omega\rangle]$.

The $F_1, J = 1/2$ state is thus pure, but for the $F_2, J = 3/2$ state there is a small $\Omega = 1/2$ character in the wavefunction, yielding a small but non-zero transition strength for the $F_2 \leftarrow F_1$ transition. The transition strength for an optical transition from state F_1, J to state F_2, J' is governed by the transition dipole moment $\mu_{JJ'}$ that follows from

$$\mu_{JJ'}|\vec{E}| = \langle F_1, J|\vec{\mu} \cdot \vec{E}|F_2, J'\rangle$$
$$= a_J b_J'\langle^2\Pi_{1/2}, J|\vec{\mu} \cdot \vec{E}|^2\Pi_{1/2}, J'\rangle$$
$$- b_J a_J'\langle^2\Pi_{3/2}, J|\vec{\mu} \cdot \vec{E}|^2\Pi_{3/2}, J'\rangle, \qquad (2)$$

where $\vec{\mu}$ is the dipole moment of the NO radical and $\vec{E}$ is the electric field of the radiation. Note that cross terms between $^2\Pi_{1/2}$ and $^2\Pi_{3/2}$ states vanish because of the $\Delta\Omega = 0$ selection rule for electric dipole allowed transitions. We define the dimensionless parameter $T_{JJ'} = \mu_{JJ'}/\mu$, where μ is the permanent dipole moment of NO ($\mu = 0.16$ D). For the $F_2, J' = 3/2 \leftarrow F_1, J = 1/2$ transition in NO, $T_{JJ'}$ takes the value 0.016.

For a two-level system in a coherent field, the transition probability $p_{JJ'}$ to transfer population from the initial state J to the final state J' is given by

$$p_{JJ'} = \sin^2\left(2\pi \frac{\mu T_{JJ'} \int |\vec{E}(t')|\mathrm{d}t'}{h}\right), \qquad (3)$$

where the integral runs over the interaction time t' between the molecule and the radiation field. In order to calculate the time dependence of the population in the initial and final states, referred to as P_{F_1} and P_{F_2}, respectively, the time structure of the FELICE pulse must be taken into account. FELICE produces a series of micropulses within a macropulse of about 10 μs duration. The shape of the micropulse is approximated by an effective square pulse. Adjacent micropulses are separated by 1 ns, and, in the particular broadband mode used, have a temporal width of 9 ps. A single micropulse has insufficient intensity to induce a transition in a substantial fraction of the NO molecules; we therefore need to include multi-pulse effects in which a series of n pulses will transfer population between the F_1 and F_2 states. We can write for the change of population ΔP_{F_2} in the upper F_2 level after n pulses:

$$\Delta P_{F_2}(n) = p_{12} \left(P_{F_1}(n) - P_{F_2}(n) \right), \qquad (4)$$

where the first and second parts on the right-hand side of the equation describe transfer of population to and from the upper F_2 state, respectively, and p_{12} follows from Equation (3). If we assume that n is a continuous variable, and furthermore assume that $P_{F_1}(n) = 1 - P_{F_2}(n)$, integration over n using the boundary conditions that $P_{F_1}(n = 0) = 1$ and $P_{F_2}(n = 0) = 0$ then yields:

$$P_{F_2}(n) = \frac{1}{2} \left[1 - e^{-2p_{12}n} \right]. \qquad (5)$$

If the transit time time of the NO beam through the FELICE beam is larger than the length of the macropulse, n equals the number of micropulses in a macropulse (9000). However if the transit time is smaller than the macropulse, n is reduced by the ratio between the transit time and the length of the macropulse. The transit time is assumed two times the waist of the FELICE optical beam divided by the velocity of the NO molecules.

From the energy in a FELICE micropulse (58 μJ), the pulse length (9 ps), the FELICE beam waist at the position of interaction (2.3 mm) and resulting focus area (16 mm^2) [20], we can estimate the electric field to be $1.7 \cdot 10^7$ V/m. The estimated velocity of the NO molecules in the beam is 550 m/s. These values result in $n = 8250$. Combining Equations (3) and (5), we estimate that the 8250 ($p_{12}n = 1.25$) micropulses are sufficient to saturate the transition, i.e. to transfer 50% of the population from the $F_1(1/2)$ level to the $F_2(3/2)$ level. This is consistent with our observation that the $F_2 \leftarrow F_1$ transition is induced under saturated conditions.

It is noted that the excitation within the free electron laser cavity, as provided by FELICE, is required to achieve saturation. Typically, the power available in the laser beam coupled out of the cavity, i.e. the FELIX laser [20], is two orders of magnitude less. In separate experiments we have tried to induce the $F_2 \leftarrow F_1$ transition using FELIX instead of FELICE. Indeed only a very marginal population transfer was observed, consistent with the estimate for the transfer probability given above. Tighter focusing of the FELIX laser into the NO beam would in principle be possible, however, the associated reduction in interaction volume would become too small to excite a significant amount of NO radicals, underlining the need for intracavity installations to excite weak molecular transitions.

4. Conclusions

We have presented the direct optical excitation of NO radicals from the $X^2\Pi_{1/2}, J = 1/2$ rotational ground state to the $X^2\Pi_{3/2}, J = 3/2$ spin-orbit excited state. This very weak spin-orbit forbidden transition at 125 cm^{-1} is induced under saturated conditions using the intracavity free electron laser FELICE. The direct optical preparation of NO radicals in the $^2\Pi_{3/2}$ state produces packets of NO radicals with almost perfect quantum state purity. In combination with the relatively large magnetic dipole moment of spin-orbit excited NO, this offers interesting prospects for the use of this benchmark molecule in deceleration and trapping experiments. The direct optical excitation demonstrated here thus effectively 'switches on' the molecule's magnetic moment, yielding interesting possibilities in experiments that aim to control interactions between samples of cold molecules. The ability to optically switch the magnetic dipole moment on or off also facilitates the accumulation of successive pulses of ground-state NO ($X^2\Pi_{1/2}$) radicals in an electric trap, subsequent to the magnetic slowing to a standstill in the $X^2\Pi_{3/2}$ state using magnetic fields [23].

ORCID

Theo Cremers http://orcid.org/0000-0002-4317-6191
Joost M. Bakker http://orcid.org/0000-0002-1394-7661

References

[1] S.Y.T. van de Meerakker, H.L. Bethlem, N. Vanhaecke and G. Meijer, Chem. Rev. **112**, 4828 (2012).

[2] H.L. Bethlem, G. Berden, F.M.H. Crompvoets, R.T. Jongma, A.J.A. van Roij and G. Meijer, Nature **406**, 491 (2000).

[3] B.C. Sawyer, B.L. Lev, E.R. Hudson, B.K. Stuhl, M. Lara, J.L. Bohn and J. Ye, Phys. Rev. Lett. **98**, 253002 (2007).

[4] N. Akerman, M. Karpov, Y. Segev, N. Bibelnik, J. Narevicius and E. Narevicius, Phys. Rev. Lett. **119**, 073204 (2017).

[5] S.Y.T. van de Meerakker, N. Vanhaecke, M.P.J. van der Loo, G.C. Groenenboom and G. Meijer, Phys. Rev. Lett. **95**, 013003 (2005).

[6] B.C. Sawyer, B.K. Stuhl, M. Yeo, T.V. Tscherbul, M.T. Hummon, Y. Xia, J. Klos, D. Patterson, J.M. Doyle and J. Ye, Phys. Chem. Chem. Phys. **13**, 19059 (2011).

[7] B.K. Stuhl, M.T. Hummon, M. Yeo, G. Quéméner, J.L. Bohn and J. Ye, Nature **492**, 396 (2012).

[8] J. van Veldhoven, J. Küpper, H.L. Bethlem, B. Sartakov, A.J.A. van Roij and G. Meijer, Eur. Phys. J. D **31**, 337 (2004).

[9] E.R. Hudson, H.J. Lewandowski, B.C. Sawyer and J. Ye, Phys. Rev. Lett. **96**, 143004 (2006).

[10] M. Brouard, D.H. Parker and S.Y.T. van de Meerakker, Chem. Soc. Rev. **43**, 7279 (2014).

[11] D.W. Chandler and S. Stolte, in *Gas Phase Molecular Reaction and Photodissociation Dynamics* (Transworld Research Network, 2007), chap. Inelastic energy transfer: The NO-rare gas system, pp. 1–63.

[12] M.H. Alexander, J. Chem. Phys. **76**, 5974 (1982).

[13] A.M. Wodtke, J.C. Tully and D.J. Auerbach, Int. Rev. Phys. Chem. **23**, 513 (2004).

[14] A.M. Wodtke, Chem. Soc. Rev. **45**, 3641 (2016).

[15] X. Wang, M. Kirste, G. Meijer and S.Y.T. vandeMeerakker, Zeitschrift für Physikalische Chemie **227**, 1595 (2013).

[16] W.L. Meerts and L. Veseth, J. Mol. Spectr. **82**, 202 (1980).

[17] X. Yang and A. M. Wodtke, J. Chem. Phys. **92**, 116 (1990).

[18] N. Bartels, B.C. Krüger, S. Meyer, A.M. Wodtke and T. Schäfer, J. Phys. Chem. Lett. **4**, 2367 (2013).

[19] B. Yan, P.F.H. Claus, B.G.M. van Oorschot, L. Gerritsen, A.T.J.B. Eppink, S.Y.T. van de Meerakker and D.H. Parker, Rev. Sci. Instrum. **84**, 023102 (2013).

[20] J.M. Bakker, V.J.F. Lapoutre, B. Redlich, J. Oomens, B.G. Sartakov, A. Fielicke, G. von Helden, G. Meijer and A.F.G. van der Meer, J. Chem. Phys. **132**, 074305 (2010).

[21] W.L. Meerts and A. Dymanus, J. Mol. Spectr. **44**, 320 (1972).

[22] G.C. Dousmanis, T.M. Sanders and C.H. Townes, Phys. Rev. **100**, 1735 (1955).

[23] S.Y.T. van de Meerakker, R.T. Jongma, H.L. Bethlem and G. Meijer, Phys. Rev. A **64**, 041401 (2001).